Compressive stress drives morphogenetic apoptosis

Tatiana Merle[1], Martine Cazales [1], Ronan Bouzignac [1], Brice Ronsin [2], Christian Rouvière [3], Magali Suzanne [1]

[1] Molecular, Cellular and Developmental Biology unit (MCD), Centre de Biologie Intégrative (CBI), Université de Toulouse, CNRS, UPS, France

[2] LITC Facility, Centre de Biologie Intégrative (CBI), Université de Toulouse, CNRS, UPS, France

Abstract

Tissues and organs are constantly submitted to physical stress, including compression, stretching, shear stress. These physical constraints can influence fundamental processes such cell division, cell death and cell differentiation. In particular, the impact of compression due to overproliferation and overcrowding has been the focus of a number of recent studies, revealing the importance of mechanics in the regulation of cell number and tissue homeostasis. However, addressing the impact of mechanical challenges in living organisms remains a challenge and how tissue compression impact cell death in the context of morphogenesis is totally unknown. Here we address this question using the drosophila leg disc as a model system. In this model, we showed that a natural compression is exerted by the surrounding tissue or envelope and that this compression is required for the correct morphogenesis of the underlying tissue, the developing leg. In this tissue, apoptosis contributes to the change in tissue shape through the generation of a pulling force on the apical surface. Apoptosis is preferentially localized in the future fold region, induced by the expression of proapoptotic genes. However, only a subset of cells expressing the proapoptotic genes are dying and how this precise pattern of cell death is established is totally unknown. Here, we found that the natural compression exerted by the envelope contributes to the precise regulation of apoptosis, the absence of compression reducing drastically the number of apoptotic events while the presence of high compression increases the number of dying cells. Thus, compression constitutes an integral part of apoptosis regulation during leg morphogenesis. We analyzed the consequences of compression on cell and nuclear geometry and found that compression affects mainly cell anisotropy and nucleus aspect ratio. We further decipher subcellular tension redistribution under compressive stress and revealed an important switch in lateral tension and opening new perspectives in term of mechanotransduction.

INTRO

Mechanobiology is a growing field of research addressing the contribution of physical parameters to living systems, including the physical properties of molecules, cells and tissues, the capability to generate and transmit forces, but also to respond to physical challenges such as shear stress, stretch or compression.

A number of pioneer studies in the field addressed the mechanical properties of isolated cells, revealing intriguing characteristic of cell mechanics, including how cell geometry can influence cortex tension and may control cell fate (Fouchard et al., 2014), the capability of cells to migrate in confined environment (Raab et al., 2016; Thiam et al., 2016) or to adapt and respond to different environmental cues on bio-functionalized substrates (Ruprecht et al., 2016). On the same line, *in vitro* studies on multicellular systems allowed to define how epithelial monolayers resist to controlled stretching (Harris et al., 2012), or how they self-organized in response to different mechanical cues from their substrate (Pérez-González et al., 2021).

It is now well recognized that tissue constraint is also an integral part of tissue homeostasis and morphogenesis. During morphogenesis, mechanics plays important functions as illustrated for example by the mechanical coupling between epidermis and muscle in c. elegans (Zhang et al., 2011), the influence of tissue stretching on growth and oriented division (Aigouy et al., 2010; Mao et al., 2013; Sagner et al., 2012), the activation of twist expression in the stomadeal primordium due to compression by the extension of the germ band (Desprat et al., 2008). However, addressing the impact of physical constraint *in vivo* is still challenging due to some limitations regarding the possibility to probe and manipulate cells and tissues without perturbing their biological function.

Epithelial tissue, which constitute a protective barrier of organs from external cues, are particularly challenged and have to deal constantly with external constraint. In epithelial cells, mechanics also constitutes an integral part of fundamental cellular processes such as cell division, which has been extensively studied (Irvine and Shraiman, 2017; Panciera et al., 2017) or cell extrusion, which was shown to be sensitive to crowding *in vitro* (Eisenhoffer and Rosenblatt, 2013; Eisenhoffer et al., 2012; Saw et al., 2017). These works showed that, in monolayer epithelium, apoptotic cell extrusion is triggered by singularities in cell alignments defined as topological defects in different epithelium types (Saw et al., 2017), and reveal that both apoptotic and live cell extrusion induced by overcrowding relies on Rho-kinase-dependent myosin contraction and the stretch-activated channel, Piezo (Eisenhoffer et al., 2012). *In vivo*, cell extrusion was shown to be increased by crowding *in vivo* in the thorax of *Drosophila* (Levayer et al., 2016; Marinari et al., 2012). Thus, cell extrusion appears to be a way to buffer external constraints through the regulation of cell number and as such responds with high sensitivity to mechanical cues. More recently, a tight link between geometrical parameters (area and relative area) and the probability to enter apoptosis was established (Cachoux et al., 2023). This work shows that cells that just divided have a high probability to enter apoptosis and identified Hippo and Notch pathways as sensors of apical surface area or differential area between neighbors, in a fast-growing tissue. While these works revealed the importance of environmental cues or cell geometry to drive cell extrusion in highly proliferative tissues and overcrowding contexts, how these observations apply to morphogenesis is totally unknown.

Here, we use an original system to address the impact of compression on morphogenetic apoptosis, the developing leg of drosophila, a tissue of cylindrical shape progressively elongating during metamorphosis. In this tissue, apoptosis is involved in the formation of stereotypic and concentric folds along the elongating leg through the generation of apico-basal forces. These forces favor the buckling of the epithelium at the level of a ring of cells with high level of apoptosis. We first show that this model has the advantage to be naturally under constraint through the compressive stress generated by the surrounding tissue, the peripodial epithelium or envelope. We further show that this compression contributes to fold formation and apoptosis regulation. Looking for factors that could favor apoptosis induction, we found that anisotropy is greatly enhanced by compression, while apical area of cells is mainly unaffected by external constraint. Finally, we observed that modulation of constraint induces dramatical changes in the subcellular distribution of membrane tension, changes that could potentially constitute new paths of apoptosis regulation.

RESULTS

I. Natural compression is required for leg morphogenesis

We first investigated whether the peripodial epithelium could exert compressive stress on the developing leg tissue as suggested by the frequent torsion of the leg during the elongation process. To

test this hypothesis, we manually removed the peripodial epithelium before the formation of the most distal fold (t4-t5) (at the beginning of metamorphosis or white pupal stage) and compare the development of the leg in the presence or absence of this surrounding tissue (see schemes in Fig1A). As soon as we removed the peripodial epithelium, we observed a sudden elongation of the tissue (see Fig1B, compare control and without peripodial epithelium conditions at t<20'), followed by a second, slower phase of elongation (see Fig1B and1C for quantifications). This sudden release reveals the existence of compressive stress exerted by the peripodial epithelium on the developing leg epithelium, compressive stress that most probably increases during leg elongation due to the limit of extension of the peripodial epithelium.

We then asked whether the release of this constraint could affect fold formation since all the fold formed in the elongating leg are formed before the opening and retraction of the peripodial epithelium. We observed that folds are less pronounced in the absence of external constraints, although some indentations can be seen after 5h of culture (Fig1D). However, these indentations never reached the depth of control folds in the absence of peripodial epithelium as shown by the quantifications of fold depth (Fig1E). Overall, these observations indicate that drosophila leg develop naturally under natural compression and that this compression exerted by the peripodial epithelium on the elongating leg are required for the correct morphogenesis of the tissue. Thus, external constraints constitute an integral part of leg morphogenesis.

II. Compression influences the apoptotic pattern

We next decided to decipher how constraints impact leg morphogenesis and fold formation. Since apoptosis was shown to constitute an important driving module of fold formation, generating an apico-basal pulling force that contributes to the increase of apical tension in the presumptive fold domain, we investigated how the apoptotic pattern evolves under different levels of constraint. To do so, we characterized apoptotic pattern in the leg disc using a sensor of apoptosis (GC3Ai; Schott et al, 2017) expressed in the apterous domain (which includes the t4-t5 fold, see scheme in Fig2A) and allowing to detect apoptosis from its initiation to the fragmentation of the cell. We then tune external constraints either by removing the natural compression exerted on the elongating leg by dissecting the surrounding peripodial epithelium (no compression) or by increasing compression and preventing leg extension through the addition of agar in the culture medium (see schemes in Fig2B). We tried different concentrations and chose a concentration of agar preventing any further elongation of the developing leg, without altering the correct development of the developing tissue. We then quantified the number of dying cells at different time points. Of note, we decided to exclude apoptotic bodies from our analysis, since these fragments (also positively marked by the apoptosensor GC3Ai) can subsist for several hours in the epithelium preventing the precise analysis of apoptotic dynamics, and quantified specifically early apoptotic cells (columnar cells positive for GC3Ai, see scheme in Fig2A). To test whether additional constraints can affect the number of apoptotic events, we cultivated the leg *ex vivo* for different periods of time and compared normal or additional compression conditions. While no significant difference was seen after 20', which correspond to the time needed to dissect the leg discs and put them in culture, a clear difference can be seen after 1h. Of note, 1h is the time required for cells that started their apoptosis before the initiation of the experiment to be fragmented, thus the columnar dying cells counted after 1h correspond to new apoptotic events. Interestingly, we observed an increase of about 50% of the number of dying cells with additional compression, compared to the control (Fig1C, D). This discrepancy is maintained at 2h30, although smaller. Altogether, these results suggest that constraint increases the number of apoptotic events. Reciprocally, we tested whether removing constraints affects the apoptotic pattern, by removing the peripodial epithelium and comparing the number of dying cells after 2h30 and 5 hours of culture. We chose this timing to avoid

counting any false positive dying cells potentially due to the delay in the execution of apoptotic events started before dissection. We observed that without constraints, the number of dying cells is 75% reduced after 2h30 (Fig2C, D). Then, after 5h, the difference got smaller between the control and the "no compression" condition. These results indicate that compression is both necessary and sufficient to induce apoptosis in this developing tissue. It further shows that compression is part of the regulation mechanism determining the pattern of apoptosis during this morphogenetic process.

III. Impact of compression on cell geometry

Since apoptosis has been shown recently as driven, at least in part, by geometrical parameters, we decided to analyze how constraint affects cell geometry during leg morphogenesis. Since leg tissue is a highly deformed tissue, we decided to use a recently developed segmentation tool adapted for automated segmentation in complex 2,5D structures called DISSECT (see Fig3A, Merle et al., 2023). In particular, it was shown that apical surface area could help predict apoptosis activation. Surprisingly, we found that cell apical perimeter and apical area are mostly unchanged in the leg disc with or without natural compression (Fig3B, C). We noticed however that anisotropy is reduced in the fold domain when natural constraint is removed. We further observed that the distribution of cell anisotropy is more dispersed when the tissue is under constraint, while in the absence of constraint, cell anisotropy is more homogeneous (Fig3D). We next characterized cell volume and cell height. Interestingly, we found that both become much more heterogeneous in the tissue under natural constraint. Particularly, while cell volume is twice as big in the segment domain, compare to the fold under natural constraint, the difference becomes non-significant between these two territories when we removed the constraint. Indeed, without natural compression, all cells adopt a rather small volume, comparable to the volume of cells from the fold domain (Fig3E, F). The same tendency is observed for the cell height, with a bigger height in the segment domain in the presence of compression, than in the fold or in the absence of compression (Fig3G). These characterizations lead us to the conclusion that, in the leg disc, probably due to the shape of the tissue, compressive stress generated by the surrounding peripodial epithelium drives a segmental pattern of cell geometry with cells getting higher and bigger in the segment, while they are smaller and more anisotropic in the fold. Surprisingly, in the absence of compression, this pattern is lost and all cells have similar height, volume and anisotropy.

In parallel, we decided to investigate whether the nuclei were impacted by the natural compression exerted on the tissue. We segmented nuclei automatically using Cell Pose (Fig3H) and extract nuclear aspect ratio and circularity. We observed that in response to a lateral compression of the epithelium, the aspect ratio was increased, while circularity was decreased on the presence of natural compressive stress (Fig3I, J).

We reasoned that this impact on cell and nucleus geometry could be due to a redistribution of tension at the level of cell membrane.

IV. Compression modifies the tension pattern and tissue dynamics

We decided to characterize and compare membrane tension in the leg disc epithelium with or without natural compression. We used a live membrane tension reporter (a planarizable push-pull fluorescent probe called FliptR for fluorescent lipid tension reporter) that can monitor changes in membrane tension by changing its fluorescence lifetime (Colom et al., 2018) and use fluorescence lifetime microscopy (FLIM) to characterize membrane tension distribution (Fig4A, B). We found that apical tension has a segmental pattern under natural compression, with a higher level of membrane tension in the fold domain than in the segment domain (Fig4C). However, this segmental pattern is

lost when compression is removed by dissecting the peripodial epithelium and membrane tension become non-significantly different between the two domains (Fig4C).

We next asked how the acto-myosin cortex was affected by compressive stress. We first characterized Myosin dynamics by FRAP experiments. We analyzed Myosin II dynamics at the apical surface of epithelial cells from the leg disc, with or without compression. We first determined the half-time recovery of Myosin-GFP (sqh-KI-GFP) with or without compression and found that there was no significative difference between both conditions, indicating that Myosin motility was mainly unaffected by compression (FigSup1). We noted however that the motile fraction was higher in the absence of constraint than in natural condition (FigSup1), suggesting that Myosin II fails to be stabilized and could be less efficient in term of cytoskeletal contraction when compression is removed. Thus, under natural compression, Myosin II become more stable apically and would accumulate preferentially in the fold domain.

On the basal part of the epithelium, on the contrary, tension is lower in the fold domain, while it is higher in the segment domain under natural compression (Fig4D). In the absence of compression, this segmental pattern is lost and basal tension become higher and more homogeneous along the whole tissue.

Altogether, this analysis points at a modification of the tension pattern in the leg disc by compressive stress, with a higher apical tension and lower basal tension in the fold than in the segment and an overall lower basal tension under natural compression.

The Hippo pathway is now well known to respond to mechanical forces (Panciera et al., 2017). It has been shown in Drosophila tissue that Ajuba could be recruited at the level of adherens junction when tension decrease due to overcrowding, leading to Wts sequestration and the export of Yorkie from the nucleus (Ibar et al., 2018; Pan et al., 2018; Rauskolb et al., 2014). More recently, it was also shown that increased basal tension could lead to a similar pathway, with the recruitment of Ajuba, Wts and the nuclear export of Yorkie (Kroeger et al., 2024). This pathway is also known to directly regulate cell survival and cell death through the activation of transcription of the apoptosis inhibitor by Yorkie (Huang et al., 2005). Finally, the translocation of Yorkie has also been shown to respond to changes in nuclear shape (Elosegui-Artola et al., 2017). Since we observed a modification of apical and basal tension distribution, as well as a modification of the aspect ratio of the nuclei under natural compression in the leg, we wondered whether the pattern of yki nuclear translocation (readout of Hippo activation) could be modified under different level of compression during the morphogenesis of the leg disc and be involved in apoptosis regulation in this tissue.

To our surprise, the intensity of nuclear Yorkie was similar in the fold and segment domains, both under natural compression or with no compressive stress (Fig 4I, J). This suggests that the segmental patterning of apical tension, with higher apical tension in the fold compared to the segment under natural compression, does not have any impact on the translocation of Yorkie in the nucleus. Another surprise was to found that Yorkie nuclear intensity was similar in the presence or in absence of compressive stress (with or without the compression exerted by the peripodial epithelium), strongly suggesting that neither the modification of apical and basal tension, nor the deformation of the nuclei were sufficient to impact Yorkie import to the nucleus in this tissue. Thus, the Hippo pathway do not seem to be involved in the regulation of apoptosis by compressive stress in this tissue and suggest that compression is controlling apoptosis through another path.

Analyzing membrane tension distribution in the leg disc, we further noticed that lateral tension was drastically modified when compression is removed. Indeed, lateral tension is clearly higher under

compression compared to “no compression” condition, suggesting that the mechanical connection between apical and basal surface is favored by compressive stress (Fig4B, E).

We wondered whether this increase in lateral tension could impact tissue reactivity. We then decided to test the capability of the tissue to contract with or without constraint. To do so, we realized laser ablation in the depth of the epithelium and follow the repair process. While there is no clear recoil, the tissue strongly contracts after damage in the control situation in order to seal the tissue (Fig4F-H). However, when the tissue is free from external compressive stress, the contraction of far less important, revealing that overall lateral dynamics is strongly perturbed (Fig4F-H).

These results interestingly point at a strong modification of lateral tension and dynamics in the leg tissue by compressive stress.

DISCUSSION

Physical constraint as a driver of apoptosis during morphogenesis

A number of mechanosensitive pathways have been identified as driver of apoptosis in tissue homeostasis, where a balance has to be established between cell proliferation and cell death. Of note, a link between apoptosis and cell division has been made recently, showing that cell division can favor subsequent apoptosis (Cachoux et al., 2023). However, how this applies to a morphogenetic context where cell division is rare and cell change shape to form a new structure, is totally unexplored. Indeed, beyond the regulation of cell number, apoptosis plays also an important role in a number of morphogenetic process and can be actively involved in shaping tissue and organ (Monier and Suzanne, 2015; Roellig et al., 2022; Toyama et al., 2008). Here, we show that the drosophila leg disc is submitted to natural compression while a series of parallel folds are formed along the elongating tissue. This natural compression is exerted by the peripodial epithelium, a surrounding tissue that resist to the elongation of the leg. Indeed, we could observe an immediate release of the leg epithelium when the peripodial epithelium was removed by manual dissection. We further showed that this natural constraint participates to the regulation of apoptosis. While increasing compression is sufficient to increase the number of apoptotic events, removing compression strongly reduced the number of cells entering apoptosis. These results show that, during morphogenesis, the regulated pattern of apoptosis is also tuned by natural compression.

Apical constraint sensing

Recently, it was shown that compression leads to an increase in apoptosis through two complementary paths in the fly thorax: either a reduction of cell surface area or of relative surface area (Cachoux et al., 2023). These two paths were shown to depends on two signaling pathways: on the one hand, regulation of apoptosis through apical surface area depends on the Hippo pathway while on the other hand, the regulation of apoptosis through the relative area of a cell compared to its neighbors depends on the Notch pathway. We thus wonder whether apical surface area could be a parameter involved in constraint sensing in our system and driving apoptosis in the fold domain. However, apical surface appears unchanged between the compressed tissue and the non-compressed one, strongly suggesting that apical area is not a sensor of constraint in this tissue. If apical area and perimeter do not seem to change much in response to compression in this tissue, we notice however that cell anisotropy was strongly affected. Of note, anisotropy has been already observed as coinciding with high apoptotic rate (Marinari et al., 2012).

Tension redistribution under compressive stress

It was shown previously that in response to overcrowding, apical junctional tension was reduced (Ibar et al., 2018; Rauskolb et al., 2014). Here, using the pupal leg disc as a model system, we analyze the distribution of membrane tension with and without natural compressive stress and revealed that apical tension become patterned along the proximo-distal axis of the leg tissue, with a higher apical tension in the fold domain, compared to the segment. Thus, contrarily to what we would expect, apical tension is not reduced. On the contrary, compression contributes to the formation of stripes that differs mechanically. This could be due to the fact that we are analyzing the effect of long-range compression by an external tissue, which may be of different strength than the one observed in response to overcrowding, suggesting that tissue can react differently to different compressive stresses.

Our work further addresses how compression impact global subcellular tension distribution, an aspect that is mostly unexplored. We could show, using the FliptR tension probe, that compressive stress has a strong impact on lateral membrane tension, which is significantly increased under the natural compressive stress exerted by the peripodial epithelium. This open new lines of investigation on how epithelial cells sense the constraints coming from their microenvironment.

The HIPPO pathway, the usual suspect for mechanically induced apoptosis

YAP (Yes-associated protein) and TAZ (transcriptional coactivator with PDZ-binding motif) are key mechanosensors and mechanotransducers controlling differentiation and proliferation in many cell types. YAP/TAZ nuclear localization can be affected by tissue mechanics in different ways, through cell-cell contact, cell–extracellular matrix contacts, cytoskeletal tension or cell shape (Panciera et al., 2017). These different signals lead to the regulation of YAP/TAZ translocation to the nucleus. In fly tissues, the YAP/TAZ homologue Yorkie nuclear translocation is also known to respond to forces (Ibar et al., 2018; Kroeger et al., 2024; Rauskolb et al., 2014). The Hippo pathway is also well-known for its key role in the control of cell growth and apoptosis (Huang et al., 2005). Altogether, this make of Hippo a perfect candidate to sense compression in the leg disc and induce apoptosis in the forming fold.

However, here we found puzzling results strongly suggesting that he hippo pathway is unsensitive to the natural compression exerted on the developing leg. Indeed, while the leg disc is submitted to natural compression during its elongation process, as shown by the release of the tissue when the peripodial epithelium is removed, the level of nuclear yorkie stays mainly the same in the presence or in the absence of compression.

Compressive stress could influence apoptosis dynamics

Apoptosis is a dynamic process relying on the activation of proteases named caspases. Caspase activation leads to the remodeling of cytoskeleton through the activation of ROCK and finally of Myosin II (Coleman et al., 2001; Croft et al., 2005; Michael et al., 2016; Monier et al., 2015). In previous works, we have shown that apoptotic cells, while dying (before fragmentation), generate an apico-basal pulling force in the depth of the epithelium, through the formation of a linear structure of acto-myosin (Ambrosini et al., 2019; Monier et al., 2015). Since we have shown here that natural compression influence Myosin stability and membrane tension pattern, it would be interesting to investigate in the next future, whether compression, beyond its impact on the induction of apoptosis, whether constraints could impact apoptosis execution and dynamics. If Myosin II stabilization is favored by lateral compression, we could expect that apoptotic force would be less efficient to deform the apical surface of the epithelium and finally the tissue. It could also have an impact on apoptosis execution,

since the apoptotic force is most probably also needed for the correct fragmentation of the cell and its proper elimination.

Finally, apoptotic cells also influence their neighbors, inducing, as a response to their own contractility, a ring of acto-myosin in the surrounding cells which participate to their extrusion (Duszyc et al., 2021; Kuipers et al., 2014; Michael et al., 2016; Ohsawa et al., 2018; Rosenblatt et al., 2001; Teng et al., 2017). Apoptosis can also contribute to tension increase in their surrounding during morphogenesis (Monier et al., 2015; Roellig et al., 2022). It would be interesting to decipher how natural compression influence this non-autonomous impact and test whether compression can favor apoptosis force transmission.

Experimental procedures

Experimental animals

The animal model used here is Drosophila melanogaster, in a context of in vivo/ex vivo experiments. In order to respect ethic principles, animals were anesthetized with CO2 (adults) before any manipulation. To avoid any release of flies outside the laboratory, dead flies were frozen before throwing them. Stocks of living flies were conserved in incubators, either at 18 or 25 degrees to maintain the flies in optimal condition. Fly food contains water, agar (0.8%), sugar (4%), flour (7.4%), yeast (2.8%), moldex (1%) and propionic acid (0.3%). Genotypes and developmental stages are indicated below. Experiments were performed in both males and females indifferently.

Drosophila Stocks

E-cadherin-GFP (w; shg{TI}-eGFP; BDSC_60584) was obtained from Bloomington Drosophila Stock Center (BDSC). sqh-eGFPKI[29B], sqh-RFPtKI[3B] and UAS-GC3Ai were previously described (Ambrosini et al, 2019; Schott et al, 2017); as well as Yorkie_KI_GFP (Fletcher et al., 2018) and alpha-spectrin::GFP (Khanna et al., 2015). Act-FRT-Stop-FRT-Gal4, His-RFP and ap^{md544}-Gal4, were obtained from Bloomington. Clones were induced in individual with the following constructions: hsFlpG5, sqh-eGFPKI[29B]; UAS-LacZ; act-FRT-Stop-FRT-Gal4, UAS-HisRFP.

Immunohistochemestry

Imaginal leg discs were dissected at white pupal stage in Schneider's insect medium (Sigma-Aldrich) supplemented with 15 % fetal calf serum and 0.5 % penicillin-streptomycin as well as 20-hydroxyecdysone at 2 mg/mL (Sigma-Aldrich, H5142), incubated for 2,5 or 5h with or without 0,4% low melting agarose. Tissues were then fixed in 4% paraformaldéhyde (PFA 4%) for 20', then extensively washed in PBT (PBS with 0.3% triton) and mounted in Vectashield (Vectors laboratories) or extensively washed in PBS-Triton 0.3%-BSA 1% (BBT) and incubated overnight at 4°C with appropriate dilutions of primary antibodies in BBT. Anti-E-cadherin antibody (Developmental Studies Hybridoma Bank – DCAD2) at 1:50 or anti-Lamin Dm0 (DSHB:ADL67.10 at 1:50). After washes in BBT, imaginal leg discs were incubated at room temperature for 2 h with 1:200 anti-rat IgG 647, anti-rat IgG 555, anti-rabbit IgG 555 or anti-mouse 555 at 1:100 (obtained from Interchim). Then, samples were washed in PBS-Triton 0.3%, suspended in Vectashield (Vectors laboratories) and mounted on slide.

Ex vivo culture of leg imaginal disc

Imaginal leg discs were dissected at white pupal stage in Schneider's insect medium (Sigma-Aldrich) supplemented with 10 % fetal calf serum and 0.6 % penicillin-streptomycin as well as 20-hydroxyecdysone at 2 mg/mL (Sigma-Aldrich, H5142). Leg discs were transferred on a slide in 12 mL of

this medium (with or without 0,4% of low melting agarose) in a well formed by a 120 mm-deep double-sided adhesive spacer (Secure-SealTM from Sigma-Aldrich). A coverslip was then placed on top of the spacer. Halocarbon oil was added on the sides of the spacer to prevent dehydration.

Peripodial epithelium removal

After dissection, leg discs were incubated with collagenase at a concentration of 1µg/L, diluted in the culture medium and heated for 5min at 37°C. Gentle micro-dissections were performed during the incubation to break the external envelope and ensure total PE removal. The incubation in collagenase never exceeded 30min. We checked that this treatment did not affected the extracellular matrix of the leg epithelium (not shown).

Confocal imaging

Samples were analyzed using a LSM880 confocal microscope fitted with a Fast Airyscan module (Carl Zeiss) and equipped with a Plan-Apochromat 40x/NA 1.3 Oil DIC UV-IR M27 objective. Z-stacks were acquired using either the laser scanning confocal mode or the High-Resolution mode (Airyscan). Airyscan Z-stacks were processed in ZEN software using the automatic strength (6 by default) and the 3D method.

Laser ablation

Laser ablation experiments were performed using a pulsed DPSS laser (532 nm, pulse length 1.5 ns, repetition rate up to 1 kHz, 3.5 mJ/pulse) steered by a galvanometer-based laser scanning device (DPSS-532 and UGA-42, from Rapp OptoElectronic, Hamburg, Germany) and mounted on a LSM880 confocal microscope (Carl Zeiss) equipped with a 63x C-Apochromat NA 1.2 Water Corr objective (Carl Zeiss). Photo-ablation in the mid-plane of the apico-basal axis of the epithelium was done by illuminating at 90 % laser power during 5s along a line. Data analysis was performed with the ImageJ software to measure tissue height before and after repair.

Quantification and statistical analysis

Nuclear segmentation

Nuclei segmentation was conducted based on immunofluorescence staining with an anti- Lamin Dm0 antibody using Cellpose with the cyto2 model, with a cell diameter set to 30 pixels and a flow threshold of 0.4. The masks were filtered using Label Size Filtering (Greater_Than; Size Limit (pixels): 8000) from the MorhoLibJ plugin in Fiji. The middle plane of each nuclei mask was extracted using a homemade macro in Fiji.

Nuclear aspect ratio and circularity

Nuclear aspect ratio and circularity were quantified using Label Analyzer (2D,3D) from the SCF-MPICBG plugin in Fiji. The assignment of nuclei to segment or fold regions was determined based on the X, Y position of the mass center of each nucleus.

Quantification of nuclear Yorkie

Utilizing the same image and segmentation parameters as those employed in the Nucleus geometry analysis, we employed Label Analyzer (2D,3D) from the SCF-MPICBG plugin in Fiji to quantify the mean nuclear signal of Yorkie (Yorkie_KI_GFP) from each nuclei mask in 3D. Then, the mean nuclear Yorkie signal was normalized by the mean grey level of the image.

Quantification of cell volume

Clones were generated in individual of the following genotype: hsFlpG5, sqh-eGFPKI[29B]; UAS-LacZ; act-FRT-Stop-FRT-Gal4, UAS-HisRFP. Random expression of UAS-LacZ was generated by 15' heat shock. The volume of individual cell was measure using the Surface tool in Imaris software.

Quantification of cell apical area, perimeter and anisotropy

The open software DISSECT (Merle et al., 2023) was used to measure automatically these parameters.

Leg elongation

Legs lengths (T1 to distal tip) were measured with the ImageJ software.

Fold formation

We measured the difference between the width of the segment T4 and the width of the forming fold T4T5. To have the fold depth, the difference is divided by 2. Mann-Whitney tests were performed with the scipy python library.

Apoptosis pattern

Legs were observed with the Imaris software and only apoptotic columnar cells were counted (i.e. still attached apically and basally). Mann-Whitney tests were performed with the scipy python library.

FRAP experiment

FRAP was performed on the LSM900 confocal microscope described above. Photobleaching was set through the bleaching module provided with ZEN software. Briefly, a rectangle region of interest (ROI) at the level of the adherens junctions was illuminated five times using a bleach dwell time with 100% 488 nm. Images were acquired every 200 ms, five times before bleaching and 250 times post-bleaching.

Flipper probe

Flipper-TR probe was diluted in DMSO at 1mM concentration and stored at -20°C. Just prior the experiment, the probe was diluted to 1µM into the leg culture medium (Schneider + ecdysone). Legs were incubated 30min in the medium and not washed for FLIM acquisitions. We used a Leica SP8 Dive biphoton equipped with a FLIM module (Falcon) for experiments, we used a 970nm pulsed laser (DeepSee Spectra-Physics) at 80MHz. We collected the t1 lifetime. For analysis, with ImageJ, a filter was applied on the lifetime images: every pixel with an intensity (photon count, other image) smaller that 1000 was discarded. Mean measurements were done with ImageJ and Mann-Whitney tests were performed with the scipy python library.

Author contributions

TM conceived and performed the experiments in fly leg discs. She also participated in article writing. **MC** set-up the conditions to cultivated leg disc with increased constraint and analyzed the apoptotic pattern in the different context of constraint. **RB** analyzed and quantified nuclei shapes using a home-made developed plug-in. **BR** help adjusting the set up for the acquisitions of the FLIM experiment. **CR** help develop Image J macro to segment nuclei. **MS** supervised the project, wrote the paper, and provided the funding.

Acknowledgement

We thank Bruno Monier for constructive comments and suggestions along the project. MS's lab is supported by grants from the National Agency of Research (ANR, PRC AAPG2021, CellPhy) and from the Research Association against Cancer (ARC, Programme Labélisé AAP2020, ARCPGA12020010001154_1591).

Figure 1

A. Removing *Drosophila* leg disc external envelope

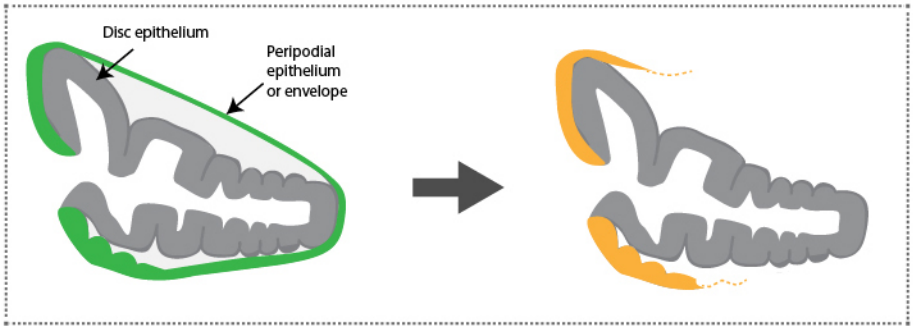

B. Leg expansion

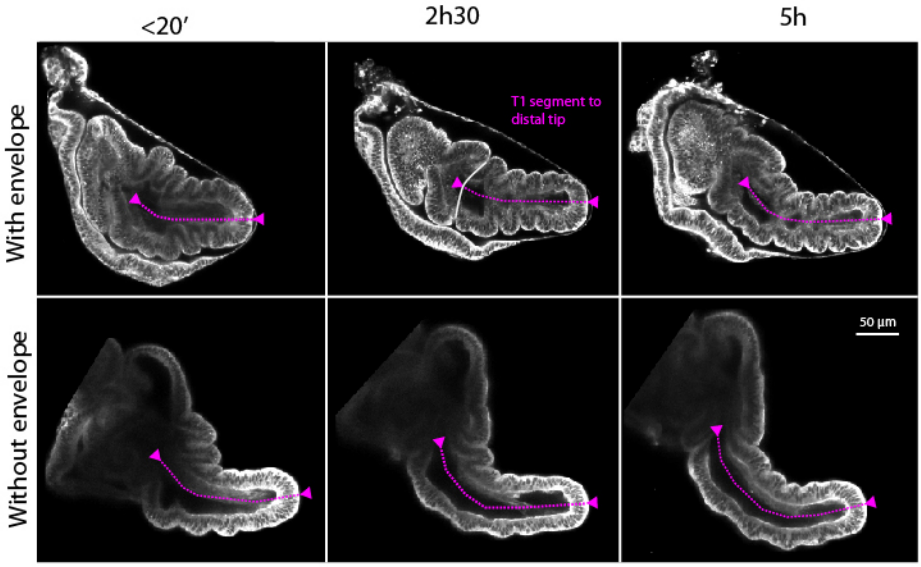

C. Quantification of leg expansion

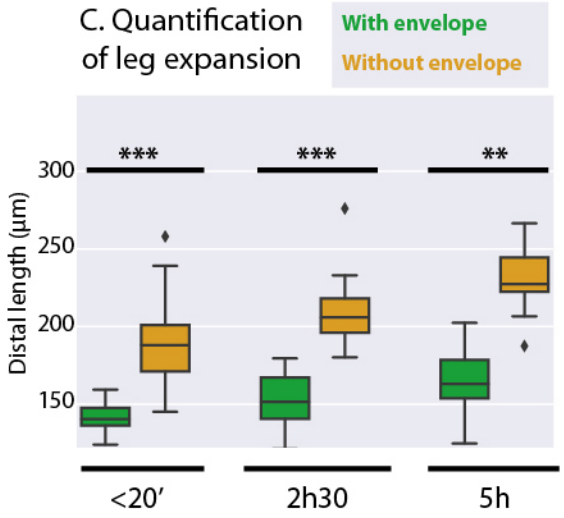

D. Fold formation

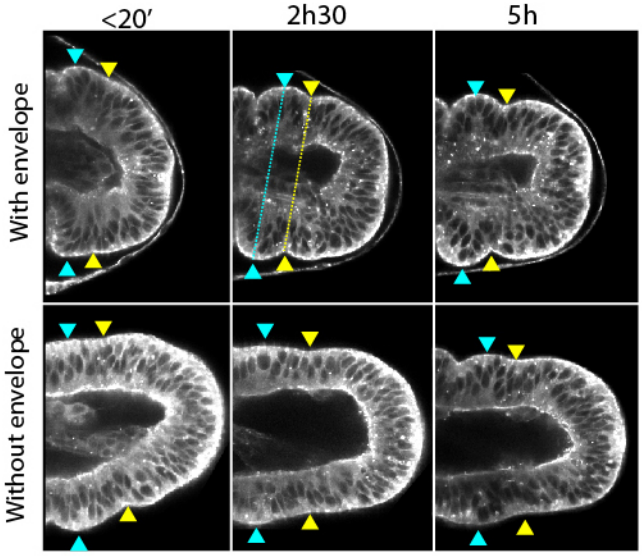

E. Quantification of fold formation

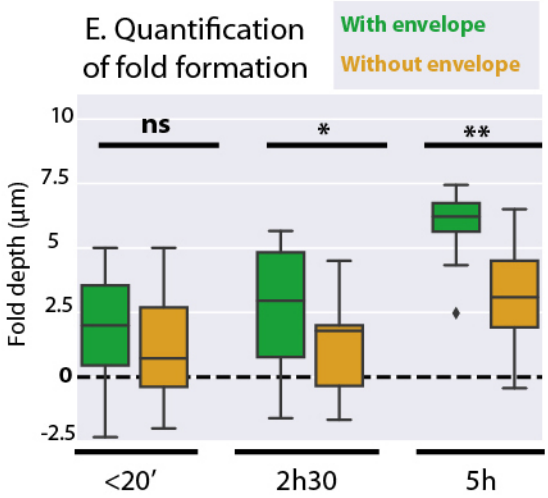

Figure 1: Compression is an integral component of morphogenesis.

A. Scheme showing the general structure of the leg disc with the thick leg disc epithelium surrounded by the thin peripodial epithelium (PE) or "envelope". PE is in green when unaltered, in yellow when microdissected. This colour code will be kept in all the figures. **B.** Still extracted from 2 movies of sqh-eGFP[KI] white pupae, showing the elongation of the leg disc in normal condition (top, with envelope) or without the envelope (bottom). **C.** Quantification of leg elongation with or without the envelope. The measured lengths are visible in magenta on images in B. **D.** Fixed samples at different time point after dissection at white pupal stage and culture ex vivo, with or without the PE. The width of the segment is measured between the cyan triangles and the width of the fold is measured between the yellow triangles. **E.** Quantification of fold formation with (top) and without (bottom) PE as shown in D.

Figure 2

A. Expression of GC3Ai in a genetically controlled domain

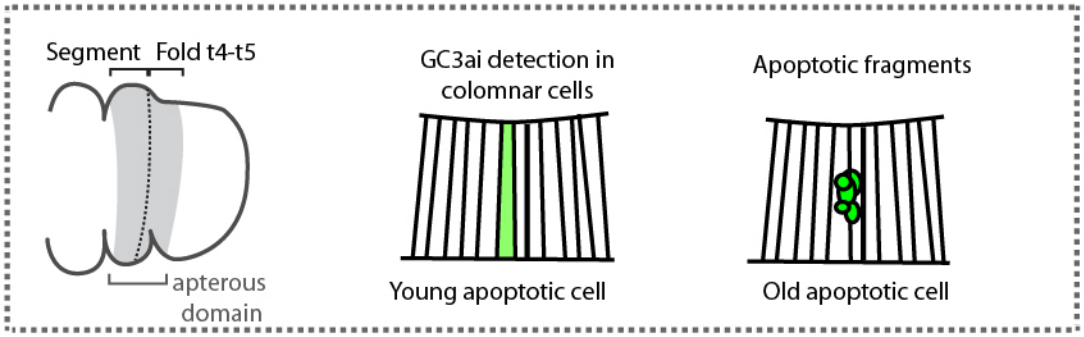

B. Incresing and decresing extermanl compressive stress applied on leg disc

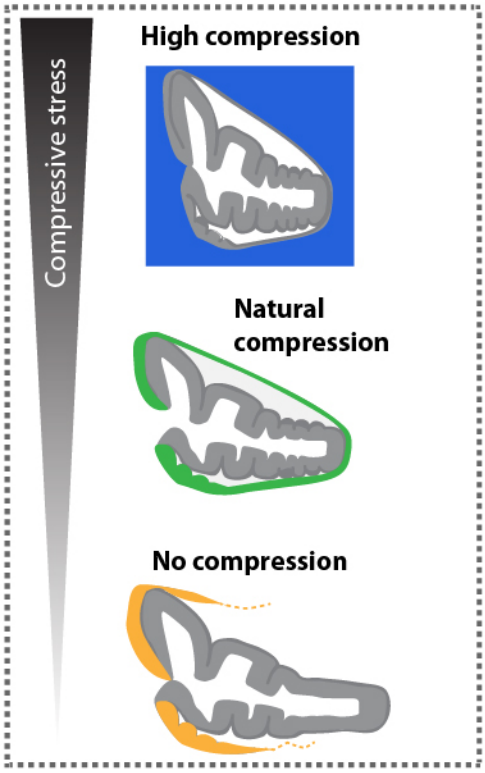

C. Apoptosis in the apterous domain according constraint at WP+2h30

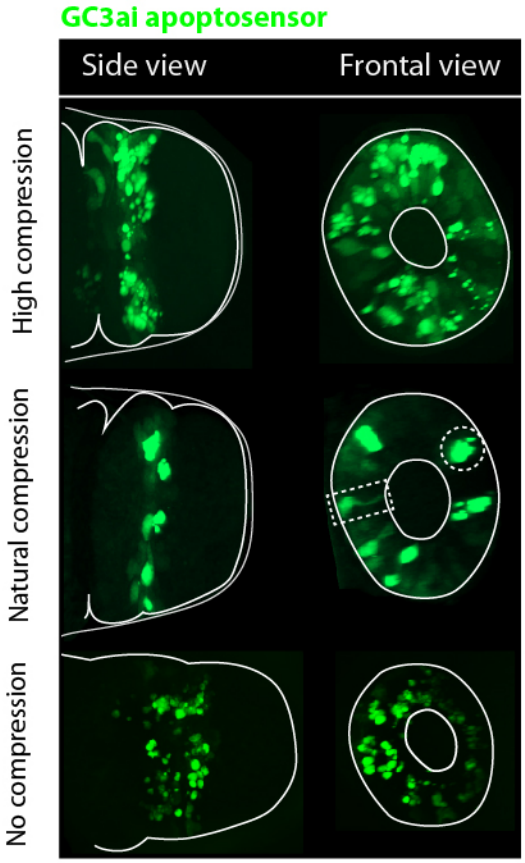

D. Number of apoptotic cells depends on compressive stress

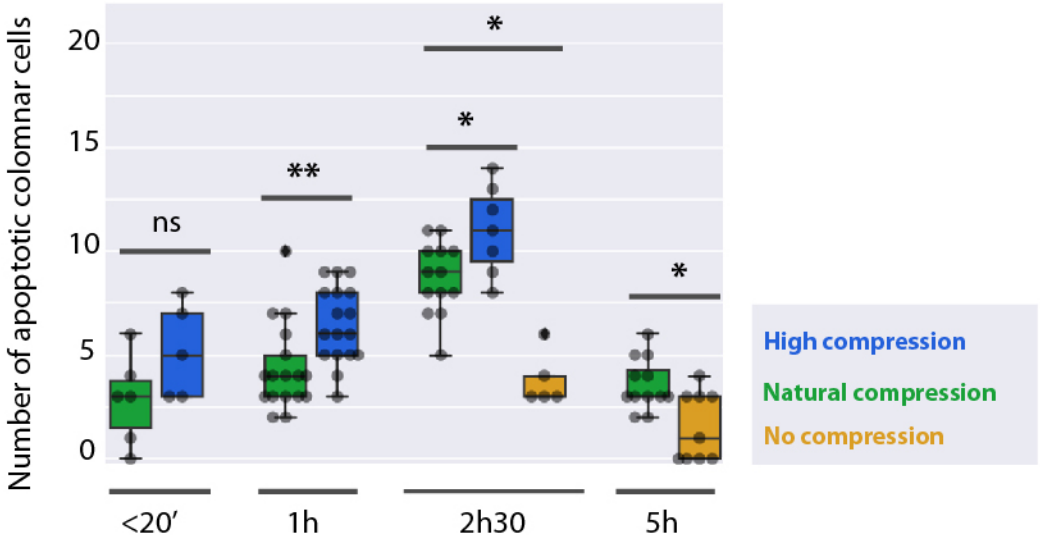

Figure 2: Natural compression drives morphogenetic cell death.

A. (left) Scheme showing the expression domain of ap in the leg disc, where the UAS-GC3Ai construct is expressed. (middle, right) Schemes showing that GC3Ai is detected both in early apoptotic cells (middle) and late apoptotic fragments (right). **B.** Schemes of the different conditions of tissue compression, going from high compression (top, blue color code), natural compression (middle, green color code) and no compression (bottom, yellow color code). **C.** Side view and frontal view of the apoptosis pattern of ap-Gal4; UAS-GC3Ai pupal leg disc cultivated with different levels of compression (high, natural and no compression). Note the difference between apoptotic fragments (circle dotted line) and columnar cell (rectangle dotted line) positive for GC3Ai. **D.** Quantification of the number of early apoptotic cells observed in the different conditions shown in C.

Figure 3

A. Cell geometry

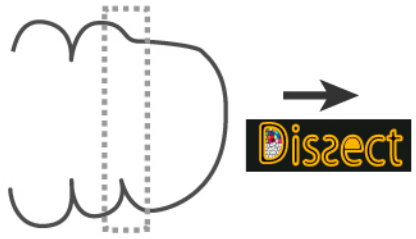

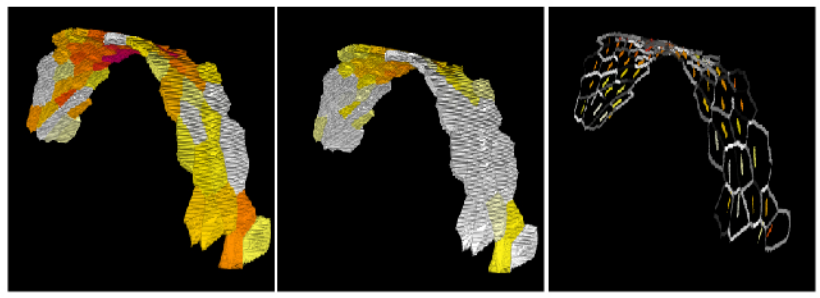

Fold segmentation and cellular parameters analysis with DISSECT

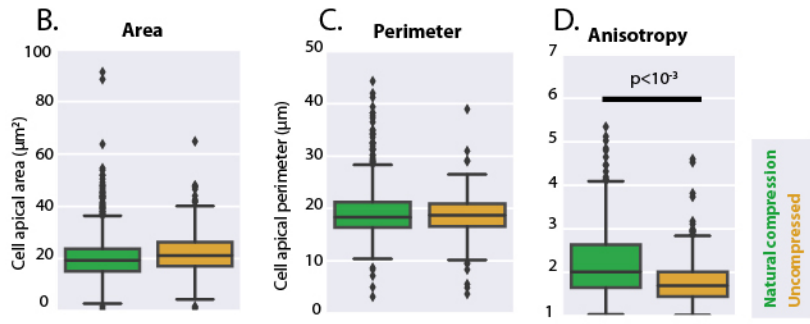

E. Single cell segmentation in 3D

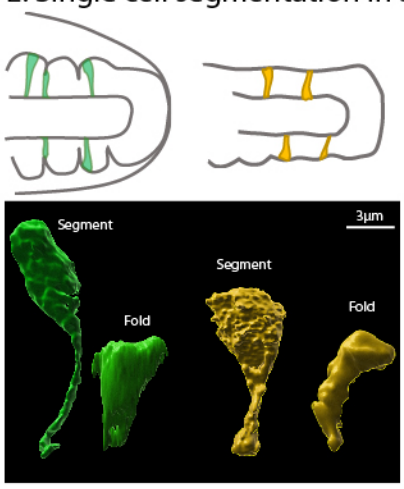

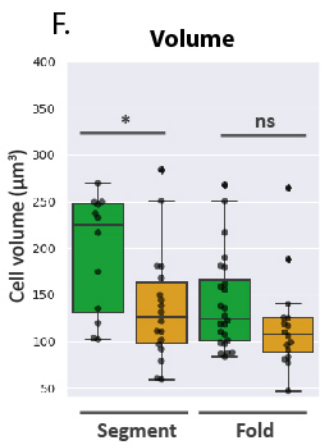

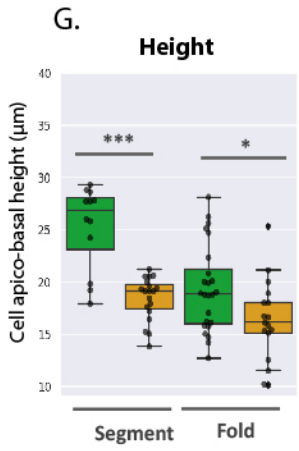

H. Nuclear segmentation

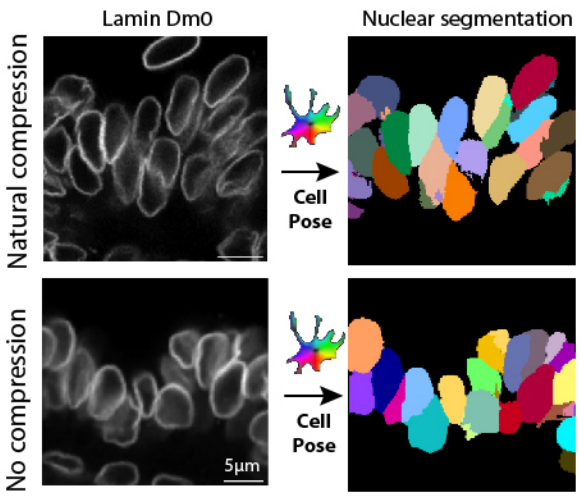

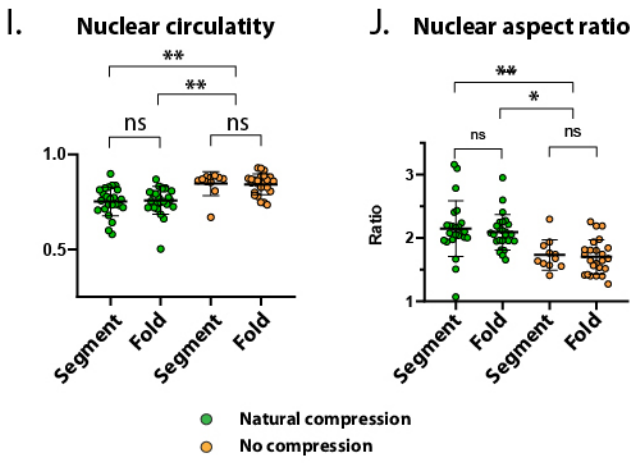

Figure 3: Impact of natural compression on cell and nucleus geometry.

A-D. Quantification of cell geometry. A. Scheme showing the part of the leg disc that has been analyzed (left) and the readout obtained from z-stack of DE-cadh::GFP pupae 2.5h after puparium formation (APF) including automatized quantification of cell geometrie parameters using the Dissect program. **B-D.** quantification of cell surface area (B), perimeter (C) and anisotropy (D). **E-G. Quantification of single cell parameter in 3D. E.** Scheme showing the principle of this single cell analysis through the random expression of UAS-lacZ construct in leg disc, with (green) or without (yellow) compressive stress. F-G. Quantification of single cell volume (F, surface in Imaris) and single cell height (G) in pupae with the following genotype: hsFlpG5, sqh-eGFPKI[29B]; UAS-LacZ; act-FRT-Stop-FRT-Gal4, UAS-HisRFP. **H-J**. **Quantification of nuclear shape. H.** Leg disc cultivated 2.5h after dissection at white pupal stage with (top) or without (bottom) natural compression, then fixed and stained with an anti-lamin Dm0 antibody. Quantification of the circularity (**I**) and the aspect ratio (**J**) in these two conditions illustrated in H.

Figure 4

A. FliptR probe

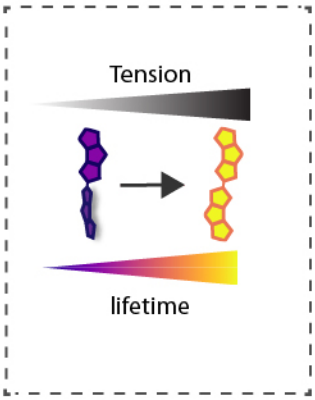

B. Membrane tension by FLIM

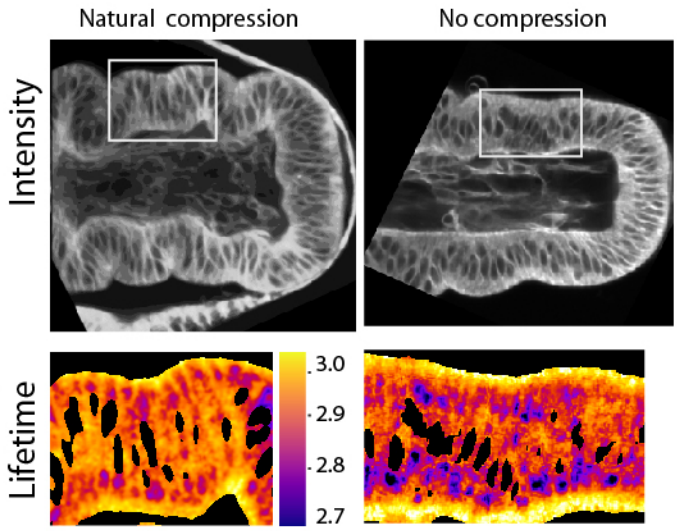

C. Apical tension

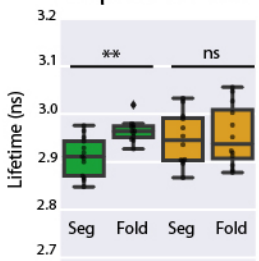

D. Basal tension

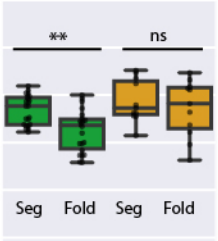

E. Lateral tension

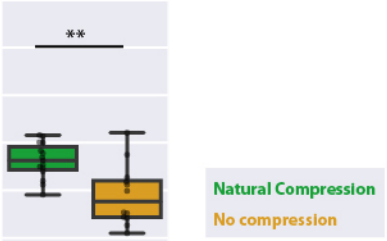

F. In depth laser ablation

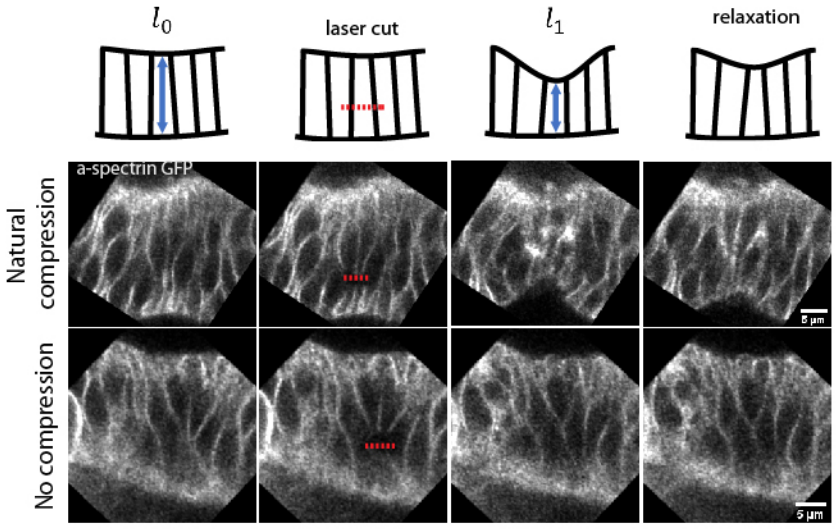

H. Normalized tissue height

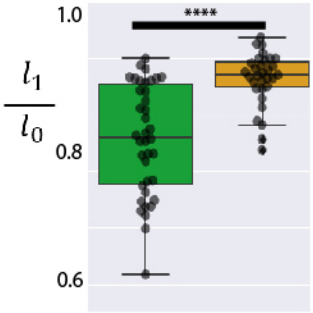

G. Height profil through time after lateral ablation

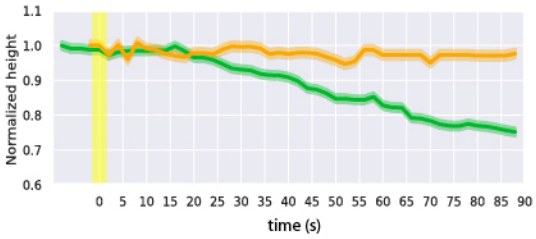

I. Yorkie

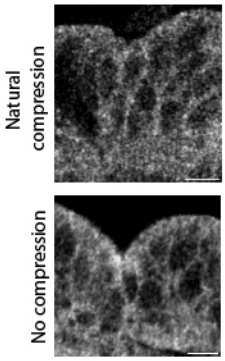

J. Nuclear Yorkie

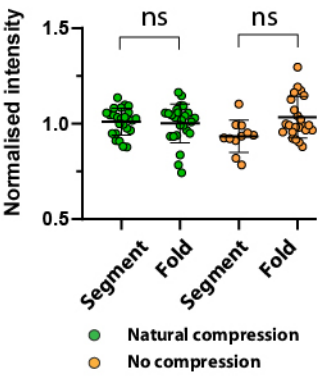

Figure 4: Impact of natural compression on subcellular membrane tension pattern.

A. Scheme from the Flipper probe showing that it changes its conformation under high membrane tension. B. Leg discs from white pupae cultivated for 2.5h with (n=10) or without PE (n=6). Raw images (top) and life time color coded (bottom). C-E. Quantification of apical (C), basal (D) and lateral (E) membrane tension with and without PE. F. In depth ablation of alpha-spectrin::GFP white pupae leg dics cultivated 2.5h with or without PE. Red dotted line indicated the site of the cut. H. Quantification of epithelium height after ablation in depth (as schematized in F). Note the strong contraction in the control situation (top). G. Representative profiles showing the evolution of epithelium height over time after ablation in depth. The green line corresponds to the control disc (with PE), while the yellow line corresponds to the disc cultivated in the absence of PE. I. Images of yki::GFP pupal leg disc, dissected at white pupal stage and cultivated 2.5h with (top) or without (bottom) PE. J. Quantification of the intensity of the yki::GFP signal in the nuclei of the corresponding leg discs.

References

Aigouy, B., Farhadifar, R., Staple, D. B., Sagner, A., Röper, J. C., Jülicher, F. and Eaton, S. (2010). Cell flow reorients the axis of planar polarity in the wing epithelium of Drosophila. *Cell* **142**, 773–86.

Ambrosini, A., Rayer, M., Monier, B. and Suzanne, M. (2019). Mechanical Function of the Nucleus in Force Generation during Epithelial Morphogenesis. *Dev Cell* **50**, 197-211.e5.

Cachoux, V. M. L., Balakireva, M., Gracia, M., Bosveld, F., López-Gay, J. M., Maugarny, A., Gaugué, I., di Pietro, F., Rigaud, S. U., Noiret, L., et al. (2023). Epithelial apoptotic pattern emerges from global and local regulation by cell apical area. *Curr Biol* **33**, 4807-4826.e6.

Coleman, M. L., Sahai, E. A., Yeo, M., Bosch, M., Dewar, A. and Olson, M. F. (2001). Membrane blebbing during apoptosis results from caspase-mediated activation of ROCK I. *Nat Cell Biol* **3**, 339–45.

Colom, A., Derivery, E., Soleimanpour, S., Tomba, C., Molin, M. D., Sakai, N., González-Gaitán, M., Matile, S. and Roux, A. (2018). A fluorescent membrane tension probe. *Nature Chem* **10**, 1118–1125.

Croft, D. R., Coleman, M. L., Li, S., Robertson, D., Sullivan, T., Stewart, C. L. and Olson, M. F. (2005). Actin-myosin-based contraction is responsible for apoptotic nuclear disintegration. *J Cell Biol* **168**, 245–55.

Desprat, N., Supatto, W., Pouille, P. A., Beaurepaire, E. and Farge, E. (2008). Tissue deformation modulates twist expression to determine anterior midgut differentiation in Drosophila embryos. *Dev Cell* **15**, 470–7.

Duszyc, K., Gomez, G. A., Lagendijk, A. K., Yau, M.-K., Nanavati, B. N., Gliddon, B. L., Hall, T. E., Verma, S., Hogan, B. M., Pitson, S. M., et al. (2021). Mechanotransduction activates RhoA in the neighbors of apoptotic epithelial cells to engage apical extrusion. *Current Biology* **31**, 1326-1336.e5.

Eisenhoffer, G. T. and Rosenblatt, J. (2013). Bringing balance by force: live cell extrusion controls epithelial cell numbers. *Trends in Cell Biology* **23**, 185–192.

Eisenhoffer, G. T., Loftus, P. D., Yoshigi, M., Otsuna, H., Chien, C.-B., Morcos, P. A. and Rosenblatt, J. (2012). Crowding induces live cell extrusion to maintain homeostatic cell numbers in epithelia. *Nature* **484**, 546–549.

Elosegui-Artola, A., Andreu, I., Beedle, A. E. M., Lezamiz, A., Uroz, M., Kosmalska, A. J., Oria, R., Kechagia, J. Z., Rico-Lastres, P., Le Roux, A. L., et al. (2017). Force Triggers YAP Nuclear Entry by Regulating Transport across Nuclear Pores. *Cell* **171**, 1397-1410.e14.

Fletcher, G. C., Diaz-de-la-Loza, M.-D.-C., Borreguero-Muñoz, N., Holder, M., Aguilar-Aragon, M. and Thompson, B. J. (2018). Mechanical strain regulates the Hippo pathway in Drosophila. *Development* **145**, dev159467.

Fouchard, J., Bimbard, C., Bufi, N., Durand-Smet, P., Proag, A., Richert, A., Cardoso, O. and Asnacios, A. (2014). Three-dimensional cell body shape dictates the onset of traction force generation and growth of focal adhesions. *Proc. Natl. Acad. Sci. U.S.A.* **111**, 13075–13080.

Harris, A. R., Peter, L., Bellis, J., Baum, B., Kabla, A. J. and Charras, G. T. (2012). Characterizing the mechanics of cultured cell monolayers. *Proc. Natl. Acad. Sci. U.S.A.* **109**, 16449–16454.

Huang, J., Wu, S., Barrera, J., Matthews, K. and Pan, D. (2005). The Hippo signaling pathway coordinately regulates cell proliferation and apoptosis by inactivating Yorkie, the Drosophila Homolog of YAP. *Cell* **122**, 421–434.

Ibar, C., Kirichenko, E., Keepers, B., Enners, E., Fleisch, K. and Irvine, K. D. (2018). Tension-dependent regulation of mammalian Hippo signaling through LIMD1. *J Cell Sci* **131**, jcs214700.

Irvine, K. D. and Shraiman, B. I. (2017). Mechanical control of growth: ideas, facts and challenges. *Development* **144**, 4238–4248.

Khanna, M. R., Mattie, F. J., Browder, K. C., Radyk, M. D., Crilly, S. E., Bakerink, K. J., Harper, S. L., Speicher, D. W. and Thomas, G. H. (2015). Spectrin tetramer formation is not required for viable development in Drosophila. *J Biol Chem* **290**, 706–715.

Kroeger, B., Manning, S. A., Fonseka, Y., Oorschot, V., Crawford, S. A., Ramm, G. and Harvey, K. F. (2024). Basal spot junctions of Drosophila epithelial tissues respond to morphogenetic forces and regulate Hippo signaling. *Dev Cell* **59**, 262-279.e6.

Kuipers, D., Mehonic, A., Kajita, M., Peter, L., Fujita, Y., Duke, T., Charras, G. and Gale, J. E. (2014). Epithelial repair is a two-stage process driven first by dying cells and then by their neighbours. *J Cell Sci* **127**, 1229–41.

Levayer, R., Dupont, C. and Moreno, E. (2016). Tissue Crowding Induces Caspase-Dependent Competition for Space. *Current Biology* **26**, 670–677.

Mao, Y., Tournier, A. L., Hoppe, A., Kester, L., Thompson, B. J. and Tapon, N. (2013). Differential proliferation rates generate patterns of mechanical tension that orient tissue growth. *EMBO J* **32**, 2790–2803.

Marinari, E., Mehonic, A., Curran, S., Gale, J., Duke, T. and Baum, B. (2012). Live-cell delamination counterbalances epithelial growth to limit tissue overcrowding. *Nature* **484**, 542–545.

Merle, T., Theis, S., Kamgoué, A., Martin, E., Sarron, F., Gay, G., Farge, E. and Suzanne, M. (2023). DISSECT is a tool to segment and explore cell and tissue mechanics in highly deformed 3D epithelia. *Dev Cell* S1534-5807(23)00364–7.

Michael, M., Meiring, J. C., Acharya, B. R., Matthews, D. R., Verma, S., Han, S. P., Hill, M. M., Parton, R. G., Gomez, G. A. and Yap, A. S. (2016). Coronin 1B Reorganizes the Architecture of F-Actin Networks for Contractility at Steady-State and Apoptotic Adherens Junctions. *Dev Cell* **37**, 58–71.

Monier, B. and Suzanne, M. (2015). The Morphogenetic Role of Apoptosis. *Curr Top Dev Biol* **114**, 335–62.

Monier, B., Gettings, M., Gay, G., Mangeat, T., Schott, S., Guarner, A. and Suzanne, M. (2015). Apico-basal forces exerted by apoptotic cells drive epithelium folding. *Nature* **518**, 245–8.

Ohsawa, S., Vaughen, J. and Igaki, T. (2018). Cell Extrusion: A Stress-Responsive Force for Good or Evil in Epithelial Homeostasis. *Developmental Cell* **44**, 284–296.

Pan, Y., Alégot, H., Rauskolb, C. and Irvine, K. D. (2018). The dynamics of Hippo signaling during Drosophila wing development. *Development* **145**, dev165712.

Panciera, T., Azzolin, L., Cordenonsi, M. and Piccolo, S. (2017). Mechanobiology of YAP and TAZ in physiology and disease. *Nat Rev Mol Cell Biol* **18**, 758–770.

Pérez-González, C., Ceada, G., Greco, F., Matejčić, M., Gómez-González, M., Castro, N., Menendez, A., Kale, S., Krndija, D., Clark, A. G., et al. (2021). Mechanical compartmentalization of the intestinal organoid enables crypt folding and collective cell migration. *Nat Cell Biol* **23**, 745–757.

Raab, M., Gentili, M., de Belly, H., Thiam, H.-R., Vargas, P., Jimenez, A. J., Lautenschlaeger, F., Voituriez, R., Lennon-Duménil, A.-M., Manel, N., et al. (2016). ESCRT III repairs nuclear envelope ruptures during cell migration to limit DNA damage and cell death. *Science* **352**, 359–362.

Rauskolb, C., Sun, S., Sun, G., Pan, Y. and Irvine, K. D. (2014). Cytoskeletal tension inhibits Hippo signaling through an Ajuba-Warts complex. *Cell* **158**, 143–156.

Roellig, D., Theis, S., Proag, A., Allio, G., Bénazéraf, B., Gros, J. and Suzanne, M. (2022). Force-generating apoptotic cells orchestrate avian neural tube bending. *Dev Cell* **57**, 707-718.e6.

Rosenblatt, J., Raff, M. C. and Cramer, L. P. (2001). An epithelial cell destined for apoptosis signals its neighbors to extrude it by an actin- and myosin-dependent mechanism. *Curr Biol* **11**, 1847–57.

Ruprecht, V., Monzo, P., Ravasio, A., Yue, Z., Makhija, E., Strale, P. O., Gauthier, N., Shivashankar, G. V., Studer, V., Albiges-Rizo, C., et al. (2016). How cells respond to environmental cues – insights from bio-functionalized substrates. *Journal of Cell Science* jcs.196162.

Sagner, A., Merkel, M., Aigouy, B., Gaebel, J., Brankatschk, M., Jülicher, F. and Eaton, S. (2012). Establishment of global patterns of planar polarity during growth of the Drosophila wing epithelium. *Curr Biol* **22**, 1296–1301.

Saw, T. B., Doostmohammadi, A., Nier, V., Kocgozlu, L., Thampi, S., Toyama, Y., Marcq, P., Lim, C. T., Yeomans, J. M. and Ladoux, B. (2017). Topological defects in epithelia govern cell death and extrusion. *Nature* **544**, 212–216.

Teng, X., Qin, L., Le Borgne, R. and Toyama, Y. (2017). Remodeling of adhesion and modulation of mechanical tensile forces during apoptosis in Drosophila epithelium. *Development* **144**, 95–105.

Thiam, H.-R., Vargas, P., Carpi, N., Crespo, C. L., Raab, M., Terriac, E., King, M. C., Jacobelli, J., Alberts, A. S., Stradal, T., et al. (2016). Perinuclear Arp2/3-driven actin polymerization enables nuclear deformation to facilitate cell migration through complex environments. *Nat Commun* **7**, 10997.

Toyama, Y., Peralta, X. G., Wells, A. R., Kiehart, D. P. and Edwards, G. S. (2008). Apoptotic force and tissue dynamics during Drosophila embryogenesis. *Science* **321**, 1683–6.

Zhang, H., Landmann, F., Zahreddine, H., Rodriguez, D., Koch, M. and Labouesse, M. (2011). A tension-induced mechanotransduction pathway promotes epithelial morphogenesis. *Nature* **471**, 99–103.